From integrator to resonator neurons: A multiple-timescale scenario

Guillaume Girier, Mathieu Desroches, Serafim Rodrigues

From integrator to resonator neurons: A multiple-timescale scenario

Guillaume Girier[1,2,*], Mathieu Desroches[2], Serafim Rodrigues[1,3]

April 21, 2023

[1] Basque Center for Applied Mathematics (BCAM), MCEN team, Bilbao, Spain.
[2] Inria Centre at Université Côte d'Azur, MathNeuro Project-Team, Sophia Antipolis, France.
[3] Ikerbasque, Basque Foundation for Science, Bilbao, Spain.
[*] Corresponding author. E-mail: ggirier@bcamath.org;

Abstract

Neuronal excitability manifests itself through a number of key markers of the dynamics and it allows to classify neurons into different groups with identifiable voltage responses to input currents. In particular, two main types of excitability can be defined based on experimental observations, and their underlying mathematical models can be distinguished through separate bifurcation scenarios. Related to these two main types of excitable neural membranes, and associated models, is the distinction between integrator and resonator neurons. One important difference between integrator and resonator neurons, and their associated model representations, is the presence in resonators, as opposed to integrators, of subthreshold oscillations following spikes. Switches between one neural category and the other can be observed and/or created experimentally, and reproduced in models mostly through changes of the bifurcation structure. In the present work, we propose a new scenario of switch between integrator and resonator neurons based upon multiple-timescale dynamics and the possibility to force an integrator neuron with a specific time-dependent slowly-varying current. The key dynamical object organising this switch is a so-called *folded-saddle singularity*. We also showcase the reverse switch via a *folded-node singularity* and propose an experimental protocol to test our theoretical predictions.

Keywords: neuronal dynamics, excitability, multiple timescales, integrator neuron, resonator neuron, folded singularities, canards.

1 Introduction

Excitable systems, in particular neurons, can be classified according to the various criteria, one of them being the existence of sub-threshold oscillations [15, 27]. This feature allows to distinguish between two types of neurons: *integrator* and *resonator*. Integrator neurons are defined by : a) the ability to get excited under high frequency pulses, b) the existence of a precise threshold, and c) the fact that they do not have a sub-threshold oscillations. They belong to what is usually referred to as type-I neuronal excitability, which means that their firing frequency starts from 0 at the transition between the stationary and the periodic regime. In contrast, resonator are neurons that : a) respond only to input with well-defined frequencies (they "resonate" with these special frequencies), b) do not

have a well-defined threshold, and c) have sub-threshold oscillations. Therefore they display type-II neuronal excitability, which means that their firing frequency is bounded away from 0 at the transition between the stationary and the periodic regimes. In an experimental framework, neurons behave either as integrators or as resonators, and this feature is observed neither simultaneously nor in the same physiological conditions.

From a dynamical systems standpoint, the underlying models of these two types of neurons differ by their bifurcation structure upon variation of an applied current I as main parameter. Namely, in integrator-type models a *saddle-node on invariant circle (SNIC)* bifurcation organises the transition from rest to spiking, and their excitability threshold is defined by the stable manifold of the saddle equilibrium that disappears through the SNIC bifurcation. In contrast, in resonator-type neuron models this transition occurs via a *Hopf bifurcation (HB)*, which is often subcritical and followed, in parameter space, by a saddle-node bifurcation of limit cycles [30]. The threshold is not well-defined however it can be approximated by a family of so-called *canard cycles* [3, 17, 8, 34].

In *in vitro* experiments, it is currently possible to make an integrator-type neuron behave like a resonator neuron by means of pharmacological intervention. Indeed, the notion of behavioural switch between integrator and resonator neuron has long been described in the experimental and computational neuroscience literature, however using different approaches. At the experimental level, the environment of the neuron can be controlled in order to obtain this change of excitable behaviour. In particular, this has been achieved pharmacologically, to control the opening of ion channels [27, 19], by current injection [11], using an electric field [35] or even by means of an excitation laser in neuromorphic experiments [10].

In mathematical and computational studies, these methods have also been demonstrated as viable [27, 10, 31, 1, 19, 35, 13], together with other approaches: to name a few, by adding terms taking into account new neuronal structures [20, 36], by varying some of the model's parameters [14, 22], or by varying the input forcing frequency [11, 25]. However, all these methods have in common that they result in changes of the system's bifurcation structure in order to allow this transition from integrator to resonator behaviour. In the present case, we want to keep the same bifurcation structure, that is, a SNIC bifurcation associated with integrator-type behaviour, and act differently upon the system so that it can be made to display the characteristic subthreshold oscillations of a resonator.

The main objective of the present work is to demonstrate mathematically that an integrator neuron – namely, a type-I neuron model– can be made to behave like a resonator neuron once an adequate slowly-varying current is applied to it with real-time feedback from the membrane potential; hence, we aim to obtain subthreshold oscillations in an integrator neuron model. Crucially, we want to achieve this apparent excitability switch without modifying the underlying bifurcation structure of the model.

To do so, we will exploit the multiple-timescale structure of the slowly-forced integrator model and show that subthreshold oscillations are possible in a specific parameter range, no matter which integrator model we are starting from, provided it has a SNIC bifurcation upon constant applied current and provided we apply to it a specific slowly-varying time-dependent current.

In a nutshell, we will show that the forcing requires to consider two additional slow variables and that the extended (minimally 4D) model possesses a so-called *folded-saddle singularity* [4, 5]. It was recently discovered [23] that subthreshold oscillations can appear near a folded saddle provided a certain algebraic condition is satisfied in the singular limit, that is, when the (explicit) timescale separation parameter ε tends to 0; see also [6]. It turns out that this condition cannot be obtained in a slowly-forced integrator system if the forcing is too simple, that is, harmonic; see Section 2. As we will show in Section 3, one needs a feedback term from the voltage in the forcing equation in order to obtain the subthreshold oscillations, which suggests in the context of real neurons, an *autaptic*

behaviour, and can be tested experimentally using a *dynamic-clamp* protocol.

We will showcase our strategy with a simple biophysical example of 2D type-I neuron model, namely the $I_{\mathrm{Na}}/I_{\mathrm{K}}$ model proposed by Izhikevich in [17]; however our approach will work with any type-I neuron model. Noteworthy, it does not require to alter the underlying bifurcation structure of the model, which is customary in studies reporting a switch from integrator to resonator. [27, 35, 13] The excitability switch that we propose here is purely due to timescale separation between the model and the forcing. We also showcase the reverse scenario, namely a switch from resonator to integrator. This requires to have a folded node instead of a folded saddle, therefore a different slow forcing structure, however here again we obtain the switch from one neuronal type to the other by staying within the same bifurcation scenario, only playing with the slow-fast structure of the model and of its folded singularity. The folded-node scenario indeed induces a particular geometry for the trajectories passing near such a folded singularity. Namely, they make transient small-amplitude oscillations, which correspond to subthreshold oscillations in the neuronal context [4, 34] and their number can be controlled, e.g., by varying initial conditions. Indeed, families of initial conditions giving rise to the same number of oscillations form so-called *rotation sectors* in phase space. Furthermore, by controlling the trajectory to flow into the first rotation sector, one can suppress these subthreshold oscillations and hence, turn the behaviour into an integrator, hence obtaining the reverse switch. However, we will argue that the folded-saddle scenario is more appropriate for this switch between integrator and resonator neuron in order to obtain a behaviour as close as possible to experiments.

This article is organised as follows. In Section 2, we present the I_{Na}/I_K model and analyse numerically its integrator structure. Then, we apply to it a first slow harmonic forcing and show that it is sufficient to create a folded-saddle singularity but insufficient to obtain subthreshold oscillations, which require a more elaborate forcing. This is why, Section 3, we adapt the forced current in order to obtain the singular-limit algebraic condition giving rise to subthreshold oscillations in the full model, and hence the resonator behaviour. In Section 4, we present the reverse scenario, whereby a resonator neuron can behave like an integrator, and show that this is due to another type of folded singularity, namely a *folded-node singularity*. Finally, we conclude in Section 5 and propose a strategy to verify experimentally our theoretical predictions.

2 Izhikevich's $I_{\mathrm{Na}}/I_{\mathrm{K}}$ model.

2.1 Under constant external current

We consider a two-dimensional conductance-based neuron model with minimal components for excitability. This model was proposed by Izhikevich in [17] and it was referred to as the $I_{\mathrm{Na}}/I_{\mathrm{K}}$ model, since it only assumes basic persistent sodium with instantaneous activation, potassium and leak currents; this is the name we shall use throughout this article. The model's equations are:

$$\begin{aligned} CV' &= I - g_{\mathrm{L}}(V - E_{\mathrm{L}}) - g_{Na} m_\infty(V)(V - E_{Na}) - g_K n(V - E_K), \\ n' &= \frac{n_\infty(V) - n}{\tau_n(V)}, \end{aligned} \tag{1}$$

with steady-state functions: $x_\infty(V) = (1 + \exp((V_{x,1/2} - V)/k_x))^{-1}$, $x = \{m, n\}$. For simplicity, we take the time constant $\tau_n(V)$ to be independent of V and we shall fix its value to 1. System (1) is based on a simplification of the two-dimensional reduction of the Hodgkin-Huxley model proposed by Krinskii & Kokoz [21], independently by Rinzel [29], and further studied, e.g., by Moehlis [24]. Thus, the variable V represents the membrane potential of the neuron, and n, the activation of potassium channels. The constants g_x

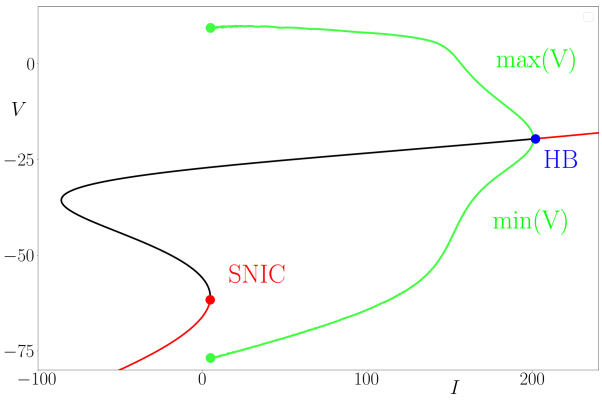

Figure 1: Bifurcation diagram of the system (1) with respect to parameter I. Red (resp. black) segments of the S-shaped curve of equilibria denote stable (resp. unstable) branches. As the applied current I is increased, oscillations (spikes) appear through a SNIC bifurcation (red dot) and then disappear through a supercritical Hopf bifurcation (blue dot denoted HB). Parameter values are: $C = 1$, $E_{\mathrm{L}} = -80$, $E_{\mathrm{Na}} = 60$, $E_{\mathrm{K}} = -90$, $g_{\mathrm{L}} = 8$, $g_{\mathrm{Na}} = 20$, $g_{\mathrm{K}} = 10$, $V_{m,1/2} = -20$, $K_m = 15$, $V_{n,1/2} = -25$, $K_n = 5$, $\tau_n(V) = 1$.

(where x corresponds to L, Na, or K) are the maximal conductances of the ionic currents considered, E_x are the Nernst potentials of the ionic species and C is the capacitance of the neural membrane; I denotes an externally applied current.

The bifurcation diagram of system (1) with respect to I, shown in Fig. 1, is typical of a neuron with type-I excitability [9]. Namely, a family of low-voltage equilibria (rest states of the neuron) destabilise and give way to a family of stable limit cycles (spiking states of the neuron) via a SNIC bifurcation, which occurs at an input current value $I \approx 4.51$. The SNIC bifurcation being a homoclinic-type bifurcation, the emerging stable cycle has a very large period (tending to infinity at the bifurcation), hence a very small frequency, which is a key hallmark of type-I excitability. At a much higher value of the input current, the branch of stable cycles disappears via a supercritical Hopf bifurcation at $I \approx 200$. Therefore, system (1) is considered to be in an integrator regime here.

2.2 Applying a slow sinusoidal external current

We now consider a periodic forcing to system (1) in the form of a slow externally-applied sinusoidal current. This can be done by replacing the constant term I in the V-equation of (1) by a time-dependent function $I(t) = I_0 + \sin(\varepsilon t)$, with $\varepsilon > 0$ a small constant. However, to further analyse the resulting periodically forced system using geometric singular perturbation theoretic tools [12], it is more appropriate to write it in autonomous form and obtain the slow sinusoidal forcing $I(t)$ as the solution of a harmonic oscillator. Hence, we consider system (1) forced by the following slow differential equations:

$$\begin{aligned} I' &= -\varepsilon J, \\ J' &= \ \ \varepsilon(I - I_0). \end{aligned} \tag{2}$$

We are therefore considering the following extended 4D system:

$$\begin{aligned} CV' &= I - g_{\mathrm{L}}(V - E_{\mathrm{L}}) - g_{\mathrm{Na}} m_\infty(V)(V - E_{\mathrm{Na}}) - g_{\mathrm{K}} n (V - E_{\mathrm{K}}), \\ n' &= \frac{n_\infty(V) - n}{\tau_n(V)}, \\ I' &= -\varepsilon J, \\ J' &= \ \ \varepsilon(I - I_0), \end{aligned} \tag{3}$$

where the prime denotes differentiation with respect to the *fast time* τ. Hence, (3) is a slow-fast dynamical system with two fast variables V and n, and two slow variables I and J. As customary in multiple-timescale dynamics, we can rescale time by a factor ε and introduce the *slow time* $t = \varepsilon\tau$, which brings the system in a different time parametrisation that will be helpful when styding its slow singular ($\varepsilon = 0$) limit, namely:

$$\begin{aligned} \varepsilon C\dot{V} &= I - g_{\mathrm{L}}(V - E_{\mathrm{L}}) - g_{\mathrm{Na}} m_\infty(V)(V - E_{\mathrm{Na}}) - g_{\mathrm{K}} n (V - E_{\mathrm{K}}), \\ \varepsilon\dot{n} &= \frac{n_\infty(V) - n}{\tau_n(V)}, \\ \dot{I} &= -J, \\ \dot{J} &= \ \ I - I_0, \end{aligned} \tag{4}$$

where the over-dot denotes differentiation with respect to t.

As long as $\varepsilon \neq 0$, the systems (3) and (4) are equivalent, they have the same phase portraits, but the solution trajectories are parameterized differently. Furthermore, their respective singular limits are different and highlight different aspects of the original system's dynamics: the fast components in the case of system (3), and the slow components for (4).

The fast singular limit (i.e., system (3) with $\varepsilon = 0$) corresponds to the original integrator $I_{\mathrm{Na}}/I_{\mathrm{K}}$ model (1), which is logical since the extended system (3) was obtained by slowly forcing this integrator model. Recall that its bifurcation structure, shown on Fig. 1, is characterised by the presence of a SNIC bifurcation. The S-shaped curve of equilibria of this fast subsystem (1) is called *critical manifold* of the full system and we label it as S^0 in Fig. 1 and subsequent figures. Its algebraic expression is given by

$$S^0 := \left\{ I - g_{\mathrm{L}}(V - E_{\mathrm{L}}) - g_{\mathrm{Na}} m_\infty(V)(V - E_{\mathrm{Na}}) - g_{\mathrm{K}} n_\infty(V)(V - E_{\mathrm{K}}) = 0 \right\} \tag{5}$$

Hence, the critical manifold, which in the present case is a surface in $\mathbb{R}^4$ (since it has the dimension of the slow variables), can be seen as a graph over V and its equation can be written $S^0 = \{I = f(V)\}$. Figure 2 shows a trajectory of the slowly forced system (3) superimposed onto the critical manifold S^0 and displayed only in the vicinity of the fast subsystem SNIC bifurcation point, for specific initial conditions of the forcing $I(0) = I_0$ and $J(0)$. The trajectory (in black, with arrows representing the direction of motion) follows the stable branch of equilibria of the fast subsystem (red branch of the parabolic-shaped bifurcation curve), which is the behaviour predicted by slow-fast theory. However, near the SNIC point – also labelled FS for reasons related to the slow subsystem (see below) – the trajectory turns around the point, instead of being repelled away, before flowing backwards as the forcing changes direction. This behaviour is counter-intuitive, it has to do with certain types of canards, and it is best explained by considering the other singular limit, namely the slow limit, of the forced integrator system (3), as we do next.

Similar to the fast subsystem, we take the $\varepsilon = 0$ limit of system (4), which provides a good approximation of the slow dynamics of the forced integrator system. However, the slow singular limit is very different from the fast one and it is given by the following

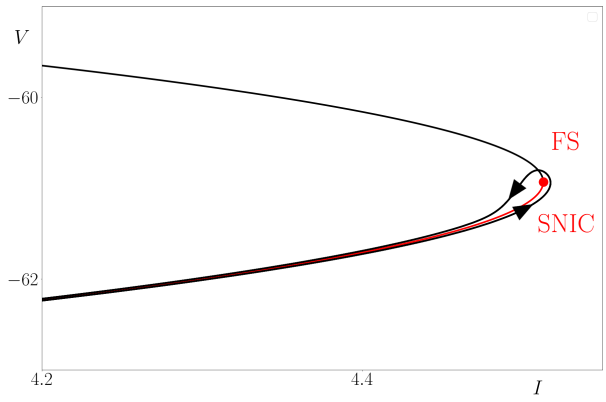

Figure 2: Folded-saddle canard trajectory (black curve with arrows) from (3) superimposed on the fast subsystem's bifurcation diagram already shown in Fig. 1. The red dot corresponds to a SNIC bifurcation point of the fast subsystem, as well as the folded-saddle singularity (FS) found in the slow subsystem; see the end of section 2.2. Black curve: unstable stationary points, red curve: stable stationary points. Parameter values are as in Fig. 1 except: $I_0 = 4$, $\varepsilon = 0.001$.

differential-algebraic system:

$$\begin{aligned} 0 &= I - g_{\mathrm{L}}(V - E_{\mathrm{L}}) - g_{\mathrm{Na}} m_\infty(V)(V - E_{\mathrm{Na}}) - g_{\mathrm{K}} n (V - E_{\mathrm{K}}), \\ 0 &= \frac{n_\infty(V) - n}{\tau_n(V)}, \\ \dot{I} &= -J, \\ \dot{J} &= \ \ I - I_0. \end{aligned} \tag{6}$$

The first two equations of (6) express the fact that in the slow singular limit, the dynamics is constrained to evolve only on S^0. In passing, this shows the importance of the critical manifold in both singular limits. The other two equations are the slow differential equations written in the slow-time parametrisation. The resulting system (6) is complicated to study as such, in particular because of the algebraic constraint which hides the limiting fast dynamics. However, one can rescue it by differentiating this algebraic constraint with respect to time which, after projecting the dynamics onto the (V, J) plane (because the slow singular dynamics is essentially 2D) and rearranging terms, yields the following version of the slow subsystem:

$$\begin{aligned} f_V(V)\dot{V} &= -J, \\ \dot{J} &= I - I_0, \end{aligned} \tag{7}$$

with $I = f(V)$ due to the constraint to evolve on S^0 and where f_V denotes the derivative of f with respect to V, namely,

$$\begin{aligned} f_V(V) = g_{\mathrm{L}} + g_{\mathrm{Na}}(m_{\infty,V}(V)(V - E_{\mathrm{Na}}) + m_\infty(V)) + \dots \\ \dots g_{\mathrm{K}}(n_{\infty,V}(V)(V - E_{\mathrm{K}}) + n_\infty(V)), \end{aligned} \tag{8}$$

with:

$$x_{\infty,V}(V) = \frac{dx_\infty(V)}{dV} = \frac{\exp\left((V_{x,1/2} - V)/k_x\right)}{k_x} x_\infty(V)^2.$$

System (7) is the more practical form of the slow subsystem or *reduced system (RS)*. This limiting system is singular along the zero set of f_V, which geometrically corresponds

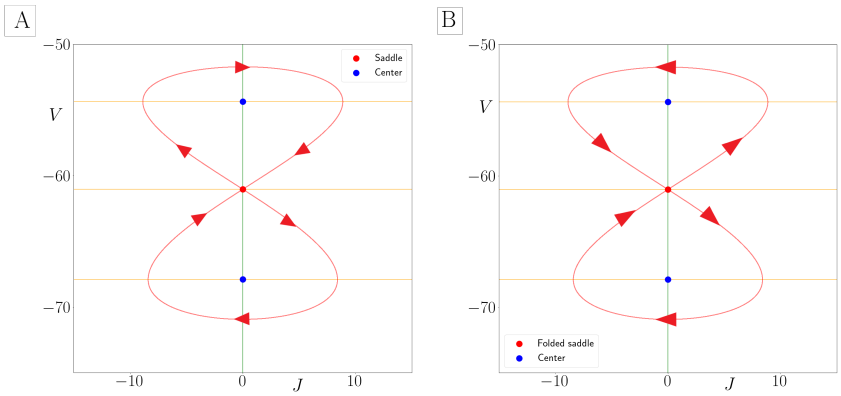

Figure 3: Phase portraits in the (J, V) plane. A: DRS system (9), B: RS system (1). In both panels, the orange lines are the components of the V-nullcline, while the green curve is the J-nullcline. A: the DRS has 3 equilibria, 2 centers (blue dots) and 1 saddle (red dot); the red curves are the stable and unstable manifolds of the saddle, they coincide and form a double homoclinic connection, each loop surrounding one of the centers. B: there are 2 center equilibria (blue dots) and one folded saddle (red dot). The red curves are the singular true and singular faux canards, they coincide to form a double folded homoclinic connection [5, 7]. Parameter values are as in Fig. 1.

to the fold set $\mathcal{F} := \{f_V(V) = 0\}$ of the critical manifold. The critical manifold of system (4) is a cubic surface and its fold set $\mathcal{F}$ has two connected components; see, e.g., Fig. 4 for an illustration of the lower fold curve F of S^0. Noteworthy, the fold curve locally separates each of the two attracting sheets of S^0, along which $f_V(V) > 0$, from the repelling sheet defined by $f_V(V) < 0$. The attractiveness and repulsiveness of S^0 is inherited from the stability and instability of equilibria of the fast subsystem (1), given that its set of equilibria precisely corresponds to S^0. For a similar reason, the fold set $\mathcal{F}$ corresponds to the set of saddle-node bifurcations of the fast subsystem, hence the lower fold curve F corresponds to a family of SNIC bifurcation points of the fast subsystem. Namely, the SNIC point shown in Fig. 1 and detected when varying parameter I in (1) does not depend on J, hence we obtain a line of such point in the forced system (4).

In order to understand the flow of the RS near the fold curve F, one classical approach is to desingularise system (7) by rescaling time by a factor $f_V(V)$, which brings forth the so-called *desingularized reduced system (DRS)*

$$\begin{aligned} V' &= -J, \\ J' &= f_V(V)(f(V) - I_0), \end{aligned} \tag{9}$$

where the prime denotes differentiation with respect to the new time, i.e., after desingularization. System (9) is now defined everywhere on $\mathbb{R}^2$ including along the fold set $\mathcal{F}$.

Two points are worth noting about the DRS. First, the change of time by a factor $f_V(V)$ artificially creates in (9) the possibility for equilibria on the fold set $\mathcal{F}$, in particular on the lower fold curve F. Such equilibria satisfy the algebraic conditions

$$J = 0,\ f_V(V) = 0,$$

whereas the other equilibria of (9) satisfy the algebraic conditions

$$J = 0,\ f(V) = I_0,$$

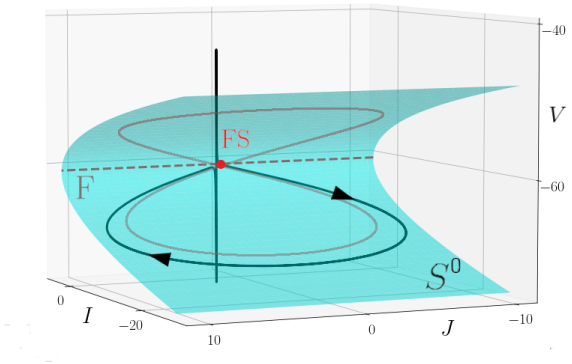

Figure 4: Phase portrait of system (3) projected onto the (I, J, V) space. Also shown is the critical manifold S^0 (blue surface), the lower fold curve F (dotted line), the singular true and faux canards (red curves), the folded-saddle singularity (red dot), labelled FS, and a trajectory making one spike without subthreshold oscillations (black curve). Parameter values are as in Fig. 1 except: $V(0) = -76$, $n(0) = 3 \cdot 10^{-05}$, $I(0) = I_0 = -5.48$ and $J(0) = 10$.

and these are also equilibria of the RS system (7). Second, the same change of time, because of the V-dependent factor, makes the orientation of trajectories of the DRS be opposite to that of the RS whenever $f_V(V) < 0$, that is, along the repelling (middle) sheet of S^0. Hence, the DRS is a standard planar dynamical system, which can for instance have a saddle equilibrium on F, and the RS has the same geometrical orbits but the reversal of orientation along the repelling sheet of S^0 implies that the saddle equilibrium of the DRS is not an equilibrium anymore in the RS. Rather, it is a special point called *folded saddle*, which two special trajectories reach in finite time and cross. One trajectory crosses it from the attracting side of S^0 upwards, continuing along the repelling side, and it corresponds to the stable manifold of the saddle equilibrium of the DRS. The other trajectory crosses it in the opposite direction and it corresponds to the unstable manifold of the saddle of the DRS. Both trajectories are related to canards in that they cross from one side to the other of the critical manifold via a folded singularity. In the folded-saddle case, they are called *true singular canard* and *faux singular canard*, respectively [4].

Figure 3 shows the phase portrait of the DRS of system (4) on panel A, and of the corresponding RS's phase portrait on panel B. A saddle equilibrium of the DRS is located on F, therefore it corresponds to a folded saddle in the RS. The DRS has two other equilibria, both of center type, they are still (true) equilibria of the RS and, hence, they will also influence the dynamics of the full system. Figure 4 shows the RS's phase portrait in a 3D (I, J, V) projection, where the critical manifold S^0 is indeed a surface and F a curve; in fact, F is a straight line here since it does not depend on J. The figure illustrates well the geometry of such problems and the role of folded-saddle singularities in shaping the dynamics of slowly periodically-forced type-I neuron models. Indeed, such systems effectively correspond to *parabolic bursters* and folded saddles organise the appearance of spikes in such bursters along solution branches in parameter space; see [5] for details.

On Fig. 4, a spiking solution of system (4) is shown on top of S^0 and it clearly appears that, as it reaches the (lower) fold curve F of S^0 and comes close to the folded-saddle point FS, the trajectory follows the true singular canard, then it makes a spike and, as the voltage is going down back to baseline, the trajectory follows the faux singular canard. Therefore in this context of type-I membrane model with slow periodic forcing, the spike-adding threshold is organised by folded-saddle canards [5]. Therefore, with a slow harmonic forcing, an integrator neuron like system (1) displays a folded-saddle singularity and still

behaves as an integrator. In particular, it cannot generate subthreshold oscillations. This is essentially due to the eigenvalue ratio of the saddle equilibrium of the DRS, as we will see next.

3 Integrator neuron with resonator behaviour

3.1 The eigenvalue ratio of the DRS's saddle equilibrium

We have just seen that the slowly forced integrator neuron model has trajectories with no subthreshold oscillations. Our aim is now to create these subthreshold oscillations in order to effectively obtain a switch from integrator to resonator behaviour.

Recent results by Mitry and Wechselberger [23], also confirmed in the context of piecewise-linear slow-fast systems in [6], show that it is possible to obtain subthreshold oscillations near a folded saddle. More precisely, near the *faux canard* of a folded saddle, which is the perturbation for $\varepsilon > 0$ small enough of the singular faux canard described in the previous section and shown in Fig. 4. As proven in [23], the algebraic condition to obtain these subthreshold small-amplitude oscillations is on the ratio μ of the eigenvalues of the saddle equilibrium of the DRS, the ratio being of the unstable eigenvalue over the stable one. Necessarily μ is negative, however if it is strictly contained between -1 and 0, then such oscillations appear around the folded saddle's faux canard; see already Fig. 5 for an illustration.

As explained in the previous section, spiking trajectories of the forced system (4) follow the singular faux canard – hence, they also stay close to its ε-perturbation, the faux canard – right after making a spike, as the voltage goes down towards baseline. Hence, provided we can obtain subthreshold oscillations near the faux canard, then these will adequately resemble those obtained in resonator neurons, which will provide us with our objective of turning an integrator neuron into a resonator one purely based on a slow-fast effect.

Now, a rapid glance at the DRS (9) makes us conclude that its Jacobian matrix has zero trace, whatever the equilibrium solution around which one linearises. Hence, the saddle equilibrium of the DRS, which corresponds to the folded-saddle of system (4), is a neutral saddle, implying that the ratio of its eigenvalues is necessarily equal to -1. This will always be the case when slowly forcing an integrator model if the forcing is harmonic. Therefore, to obtain subthreshold oscillations one needs to consider a more elaborate forcing, namely one that includes a feedback term from the voltage.

3.2 Slow forcing with feedback from the voltage

We now consider a more general forcing, with a feedback term in V in the I equation in order to obtain a non-zero trace in the Jacobian matrix of the new DRS evaluated at the saddle equilibrium of interest. We will keep the J equation only dependent on I as we simply need one non-zero diagonal element in the Jacobian matrix evaluated at this saddle equilibrium in order to ensure that its eigenvalue ratio will be different than -1. For simplicity, we will keep the dependence in V in the I equation linear and show that it suffices to obtain the expected behaviour both at the level of the eigenvalue ratio and in the full system's solutions. Specifically, we define the new slow forcing (written in fast time) as

$$\begin{aligned} I' &= \varepsilon\,(-J + \alpha V)\,, \\ J' &= \varepsilon\ \ (I - I_0), \end{aligned} \tag{10}$$

which then yields the new DRS (after rescaling to the slow time)

$$\begin{aligned} V' &= -J + \alpha V, \\ J' &= f_V(V)(f(V) - I_0). \end{aligned} \tag{11}$$

Note that the voltage equation of the DRS is obtained from the slow differential equation for I in the forcing system, and that I must be kept equal to $f(V)$ in the slow singular limit. For these reasons, it would suffice that the I equation of the forcing depends on I and not on V, on top of its J dependence, in order to obtain a non-zero trace in the Jacobian matrix of the DRS corresponding to this new forcing. This would amount to replacing V by I in the first equation of (11). As a consequence, this in particular would avoid to use a feedback term in V in the full system (10). However, it turns out that the full dynamics would not be able to exploit within its spiking regime the eigenvalue ratio of the slow singular limit, as additional unwanted equilibria would arise.

Therefore we keep the new slow forcing system (10) to obtain the resonator behaviour. This new forcing may appear for now as the result of some *ad hoc* reverse engineering process, however we shall propose in the discussion section an explanation for its form and a possible experimental implementation of it.

We can now verify that the new DRS (11) does possess a saddle equilibrium on F and that one can take a value of parameter α so that its eigenvalue ratio is strictly between -1 and 0. At an equilibrium (V^*, J^*) located on the lower fold curve F of S^0, the Jacobian matrix of (11) reads

$$\mathbf{J} = \begin{pmatrix} \alpha & -1 \\ f_{VV}(V^*)(f(V^*) - I_0)) & 0 \end{pmatrix},$$

where $f_{VV}(V)$ is the second derivative of f with respect to V. Given that α contributes to the trace of $\mathbf{J}$ and not to its determinant, it is clear that we still have a saddle equilibrium on F, and hence a folded saddle in the full system with the new forcing. Therefore, the eigenvalue ratio μ is given by

$$\mu = \frac{\alpha + \sqrt{\alpha^2 - 4 f_{VV}(V^*)(f(V^*) - I_0)}}{\alpha - \sqrt{\alpha^2 - 4 f_{VV}(V^*)(f(V^*) - I_0)}}. \tag{12}$$

We then verify numerically that, for α negative and sufficiently large in absolute value, μ is indeed strictly between -1 and 0. For instance, by fixing $\alpha = -4$ one can observe the expect subthreshold oscillations when simulating the full system, as illustrated in Fig. 5 where we also show the critical manifold S^0 (blue surface), its lower fold curve F (dotted line), the folded-saddle singularity, labelled FS (red dot), and the two singular canards

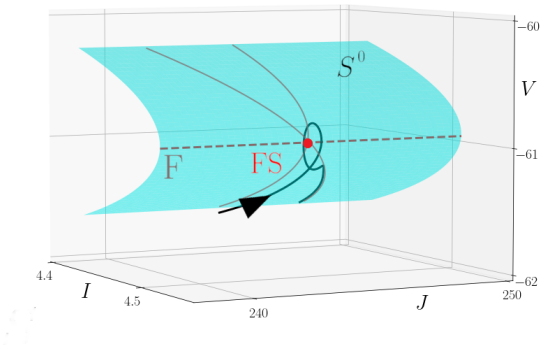

Figure 5: Phase portrait of system (4) projected onto the (I, J, V) space. Also shown at the critical manifold S^0 (blue surface), the lower fold curve F (dotted line), the singular true and faux canards (red curves), the folded-saddle singularity (red dot), labelled FS, and a trajectory making subthreshold oscillations (black curve). Parameter values are as in Fig. 1 except for the new parameter α: $\alpha = -4$.

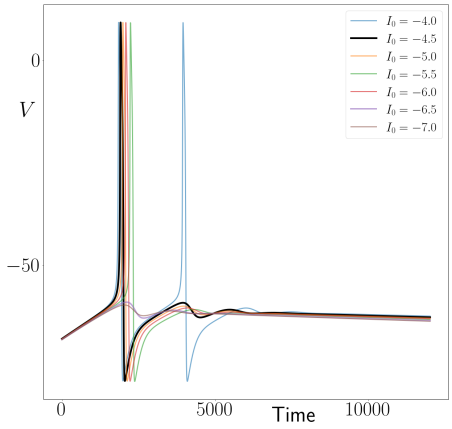

Figure 6: Integrator neuron (1) acting as a resonator with the slow forced current (10). Parameter values are as in Fig. 5 except : $\varepsilon = 0.02$, $\alpha = -8$, $V(0) = -113.11$, $n(0) = 3 \cdot 10^{-05}$, $J_0 = 546$, and $I(0) = I_0$ ranging between -4 and -7.

(red curves traced on S^0). Any values of α such that μ in expression (12) is between -1 and 0 will work equally well. The plotted trajectory is entirely subthreshold, however it comes close to the folded saddle and then turns back; as the voltage is going down towards baseline, it oscillates around the singular faux canard. Hence we have obtained a key feature of a resonator neuron by simply modifying the slow forcing received by an *a priori* integrator neuron without modifying its bifurcation structure obtained with constant forcing. Resonator models have also other features which we can as well recover here.

In Figure 6, we highlight this resonator effect in the time series of the full system with the new forcing, obtained by taking an ensemble of initial conditions for the forcing, namely varying I_0. What we observe is a transition in the voltage response from no spike, to one spike and then two spikes, depending on the value of I_0. Every trajectory with at least one spike has clear subthreshold oscillations after the spike, or after the second spike for trajectories that have two spikes. What is more, the values of I_0 at which we observe a first spike in the voltage response, and then a second spike, are quite specific. This confirms that the forced system resonates with specific inputs. Consequently, we have obtained the main features of a resonator neuron. Again, the main mechanism behind this switch of behaviour is purely due to the slow forcing received by the integrator model, and based upon multiple-timescale dynamical phenomena.

4 A multiple-timescale scenario for the reverse switch: from resonator to integrator

So far, we have mostly focused on the switch from an integrator to a resonator while retaining the characteristics of the integrator in absence of forcing. It is also possible to obtain the reverse switch, that is, to have a resonator neuron that behaves like an integrator. To do so, we keep system (1) but now consider yet another slow forcing, namely:

$$\begin{aligned} I' &= \varepsilon \left(-\beta J + \alpha(V - V_0)\right), \\ J' &= \varepsilon \ \ (I - I_0), \end{aligned} \tag{13}$$

where β is a new parameter that allows us to regulate the applied current; β was implicitly

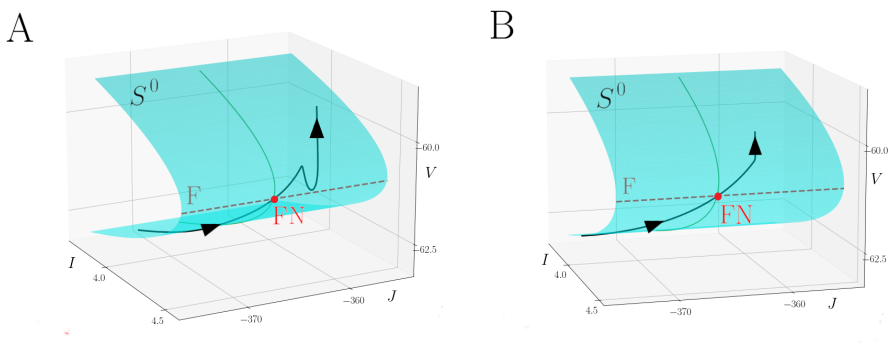

Figure 7: A: Resonator neuron model (1) with the slow forced current (13) for $J(0) = -370$. The folded node is labelled FN. B: Same model acting as an integrator for $J(0) = -380$, $I(0) = -6.0$. Parameter values are as in Fig. 5 except for the new parameter β: $\beta = -1$, and $V(0) = -65.933$.

equal to 1 in the previous slow forcing (10). We also add V_0 as new parameter as it helps controlling the amplitude of the feedback term from the voltage; V_0 was implicitly equal to 0 in the previous slow forcing. The new parameter β also enables to change the type of folded singularity by changing the topological type of the DRS equilibrium located on the fold curve F. In particular, varying β may turn the saddle into a node, hence giving a folded node in the full system. The non-singular ($\varepsilon > 0$ small) dynamics near a folded node is well known to produce small oscillations, which in the neuronal context correspond to subthreshold oscillations [4]. Also known is the fact that, near a folded node, the phase space is locally partitioned into rotation sectors in which trajectories make a fixed number of subthreshold oscillations. Hence, it suffices to take initial conditions into the first rotation sector in order to obtain that the dynamics of this resonator system appears to behave like an integrator; Fig. 7 illustrates this effect.

Therefore, it is interesting to showcase this effect of a resonator that behaves like an integrator without changing anything to its structure. However, the observed behaviour has a notable discrepancy with standard resonator neurons, whereby the subthreshold oscillations occur before the spike and not after; see Fig. 7 A. Yet, this type of scenario can be related to experimental observations since there are neurons with this kind of electrical behaviour recorded *in vitro*; see [2] for an example in dorsal root ganglion neurons of rats.

5 Conclusion

In this work, we have studied a novel mechanism for excitability switch, from integrator to resonator and *vice versa*, within the framework of multiple-timescale dynamical systems. As a proof-of-concept, we considered the simple yet biophysical 2D example of the I_{Na}/I_K model by Izhikevich, but it would work just as well in any type-I model. Starting from a parameter set in which the model behaves as an integrator in the classical sense, that is, where the spiking regime occurs through a SNIC bifurcation, we first applied a slow periodic forcing in order to create a multiple-timescale structure in the forced model, and to show that the resulting 4D model possesses a folded-saddle singularity. Following standard geometric singular perturbation theory (GSPT), we derived the desingularized reduced system (DRS) and showed that it had a saddle equilibrium on the fold curve of the critical manifold of the original system. This slow periodic forcing preserved the integrator behaviour. However, modifying the forcing by including a feedback term from the membrane potential, we managed to affect the eigenvalues of the saddle equilibrium

of the DRS. This, according to recent results from GSPT [23], has the effect to allow for small-amplitude oscillations in trajectories that pass near the folded saddle. In turn, this provided us with a mechanism to obtain subthreshold oscillations in a neuron model that was *a priori* an integrator, hence making it behave like a resonator. The feedback term in V in the slow current forcing can be seen as a simple form of *autaptic* connection, which is physiologically plausible.

Therefore, we can see these results as theoretical predictions that we would like to verify experimentally. From the standpoint of electrophysiological measurements on real neurons, the possibility to apply a current that depends in real time on the readout potential from the neuron can be obtained through a *dynamic-clamp* protocol [26, 32]. The experimental setup allows to inject currents to a cell that depends upon the measured voltage in real time. It can be used in conjunction with pharmacological blockade of e.g. one ionic channel of the cell and injecting back the corresponding current as a result of a computer simulation using the measured voltage. We are current working on validating our theoretical prediction using dynamic-clamp experiments.

From the modeling's point of view, adding this term αV in the slow differential equation of the forcing current was a way to modulate the determinant of the Jacobian matrix of the DRS, and therefore obtain subthreshold oscillations after a spike as well as modulate their number. Thus, it is possible to keep the bifurcation structure and the characteristics of an integrator neuron model while forcing it to display the specific behaviour of a resonator neuron.

This difference with the classical scenario of integrator neuron models can potentially have interesting fallouts in the study of information transmission between neurons. Indeed, by definition, an integrator neuron integrates the message and returns to the rest electrical potential without subthreshold oscillation. The fact that an integrator neuron can resonate like a resonator neuron shows that the transmission of information is more complex than a simple integration of a message given upstream. This is an interesting avenue for follow-up research on this topic.

We have also shown that the inverse scenario of switch from a resonator towards an integrator is also possible, by using a folded-node scenario in place of a folded-saddle one. However, the subthreshold oscillations obtained with a folded-node scenario occur before the spike rather than after, which is uncommon for resonator neurons. This may be associated with certain types of neurons (as reported in e.g. [2]) and to the dynamical phenomenon of *mixed-mode oscillations (MMOs)* [4]. The most important aspect of this numerical experiment is that the resonance phenomenon does occur and it can be related to known properties of folded-node canards, in response to specific forcing inputs [33]. Yet, one can control the trajectories in such a scenario so that no subthreshold oscillation occurs as the solution flows past the folded node, which effectively makes the resonator behave like an integrator. We plan to verify experimentally this theoretical and computational prediction, first in neuromorphic analog circuits and then, using dynamic clamp, in real neurons.

6 Acknowledgments

SR was supported by Ikerbasque (The Basque Foundation for Science); GG and SR acknowledges support from the Basque Government through the BERC 2022-2025 program and by the Ministry of Science and Innovation: BCAM Severo Ochoa accreditation CEX2021-001142-S / MICIN / AEI / 10.13039/501100011033 and through project RTI2018-093860-B-C21 funded by (AEI/FEDER, UE) and acronym "MathNEURO". MD and SR acknowledge the support of Inria via the Associated Team "NeuroTransSF".

References

[1] Isam Al-Darabsah and Sue Campbell. M-current induced bogdanov–takens bifurcation and switching of neuron excitability class. *The Journal of Mathematical Neuroscience*, 11, 02 2021.

[2] Ron Amir, Martin Michaelis, and Marshall Devor. Burst discharge in primary sensory neurons: Triggered by subthreshold oscillations, maintained by depolarizing afterpotentials. *The Journal of Neuroscience*, 22:1187–1198, 02 2002.

[3] Eric Benoît, Jean-Louis Callot, Francine Diener, and Marc Diener. Chasse au canard. *Collectanea Mathematica*, 32(1-2):37–119, 1981.

[4] M. Desroches, J. Guckenheimer, B. Krauskopf, C. Kuehn, H. M. Osinga, and M. Wechselberger. Mixed-Mode Oscillations with Multiple Time Scales. *SIAM Review*, 54(2):211–288, January 2012.

[5] M. Desroches, M. Krupa, and S. Rodrigues. Spike-adding in parabolic bursters: The role of folded-saddle canards. *Physica D: Nonlinear Phenomena*, 331:58–70, 2016.

[6] Mathieu Desroches, Antoni Guillamon, Enrique Ponce, Rafael Prohens, Serafim Rodrigues, and Antonio E Teruel. Canards, folded nodes, and mixed-mode oscillations in piecewise-linear slow-fast systems. *SIAM review*, 58(4):653–691, 2016.

[7] Mathieu Desroches and Vivien Kirk. Spike-adding in a canonical three-time-scale model: superslow explosion and folded-saddle canards. *SIAM Journal on Applied Dynamical Systems*, 17(3):1989–2017, 2018.

[8] Mathieu Desroches, Martin Krupa, and Serafim Rodrigues. Inflection, canards and excitability threshold in neuronal models. *Journal of Mathematical Biology*, 67(4):989–1017, 2013.

[9] Bard Ermentrout. Type I membranes, phase resetting curves, and synchrony. *Neural computation*, 8(5):979–1001, 1996.

[10] Johannes Feldmann, Nathan Youngblood, C David Wright, Harish Bhaskaran, and Wolfram HP Pernice. All-optical spiking neurosynaptic networks with self-learning capabilities. *Nature*, 569(7755):208–214, 2019.

[11] Jean-Marc Fellous, Arthur Houweling, R Modi, Rajesh Rao, Paul Tiesinga, and Terrence Sejnowski. Frequency dependence of spike timing reliability in cortical pyramidal cells and interneurons. *Journal of neurophysiology*, 85:1782–7, 05 2001.

[12] Neil Fenichel. Geometric singular perturbation theory for ordinary differential equations. *Journal of Differential Equations*, 31(1):53–98, 1979.

[13] Raul Guantes and Gonzalo Polavieja. Variability in noise-driven integrator neurons. *Physical review. E, Statistical, nonlinear, and soft matter physics*, 71:011911, 02 2005.

[14] Bruce Hutcheon and Yosef Yarom. Resonance, oscillation and the intrinsic frequency preferences of neurons. *Trends in Neurosciences*, 23:216–222, 06 2000.

[15] E. M. Izhikevich. Neural excitability, spiking and bursting. *International Journal of Bifurcation and Chaos*, 10(06):1171–1266, 2000.

[16] Eugene M Izhikevich. Resonate-and-fire neurons. *Neural networks*, 14(6-7):883–894, 2001.

[17] Eugene M Izhikevich. *Dynamical Systems in Neuroscience*. MIT press, Cambridge, MA (USA), 2007.

[18] Eugene M Izhikevich and Frank Hoppensteadt. Classification of bursting mappings. *International Journal of Bifurcation and Chaos*, 14(11):3847–3854, 2004.

[19] Christoph Kirst, Julian Ammer, Felix Felmy, Andreas Herz, and Martin Stemmler. Fundamental structure and modulation of neuronal excitability: Synaptic control of coding, resonance, and network synchronization.

[20] Christoph Kirst, Andreas Herz, and Martin Stemmler. From integrator to resonator: The effect of dendritic geometry on neuronal excitability. *Frontiers in Computational Neuroscience*, 2, 01 2008.

[21] VI Krinskiĭand Iu M Kokoz. Analysis of the equations of excitable membranes. i. reduction of the hodgkins-huxley equations to a 2d order system. *Biofizika*, 18(3):506–511, 1973.

[22] Olivier Macherey, Robert Carlyon, Astrid van Wieringen, and Jan Wouters. A dual-process integrator–resonator model of the electrically stimulated human auditory nerve. *Journal of the Association for Research in Otolaryngology : JARO*, 8:84–104, 04 2007.

[23] J. Mitry and M. Wechselberger. Folded saddles and faux canards. *SIAM Journal on Applied Dynamical Systems*, 16(1):546–596, 2017.

[24] Jeff Moehlis. Canards for a reduction of the hodgkin-huxley equations. *Journal of mathematical biology*, 52:141–153, 2006.

[25] Raul Muresan and Cristina Savin. Resonance or integration? self-sustained dynamics and excitability of neural microcircuits. *Journal of neurophysiology*, 97:1911–30, 04 2007.

[26] H. Ori, H. Hazan, E. Marder, and S. Marom. Dynamic clamp constructed phase diagram for the hodgkin and huxley model of excitability. *Proc. Natl. Acad. Sci. USA*, 117:3575, 2020.

[27] Steven Prescott, Stephanie Ratté, Yves Koninck, and Terrence Sejnowski. Pyramidal neurons switch from integrators in vitro to resonators under in vivo-like conditions. *Journal of neurophysiology*, 100:3030–42, 11 2008.

[28] J. Rinzel. A formal classification of bursting mechanisms in excitable systems. In *International Congress of Mathematicians, Berkeley, California, USA, August 3-11, 1986*, volume II, pages 1578–1593, Providence, RI (USA), 1987. American Mathematical Society.

[29] John Rinzel. On repetitive activity in nerve. *Federation proceedings*, 37(14):2793–2802, 1978.

[30] John Rinzel and G Bard Ermentrout. Analysis of neural excitability and oscillations. In Christof Koch and Idan Segev, editors, *Methods in neuronal modeling, Second Edition*, volume 2, pages 251–292. 1998.

[31] James Roach, Bolaji Eniwaye, Victoria Booth, Leonard Sander, and Michal Zochowski. Acetylcholine mediates dynamic switching between information coding schemes in neuronal networks. *Frontiers in Systems Neuroscience*, 13, 11 2019.

[32] A. A. Sharp, M. B. O'Neil, L. F. Abbott, and E. Marder. Dynamic clamp: computer-generated conductances in real neurons. *J. Neurophysiol.*, 69:992, 1993.

[33] Martin Wechselberger. Existence and bifurcation of canards in \mathbbrˆ3 in the case of a folded node. *SIAM Journal on Applied Dynamical Systems*, 4(1):101–139, 2005.

[34] Martin Wechselberger, John Mitry, and John Rinzel. *Canard Theory and Excitability*, volume 2102, pages 89–132. 11 2013.

[35] Guosheng Yi, Jiang Wang, Xile Wei, Kai-Ming Tsang, Wai-Lok Chan, Bin deng, and Chun-Xiao Han. Exploring how extracellular electric field modulates neuron activity through dynamical analysis of a two-compartment neuron model. *Journal of computational neuroscience*, 36, 09 2013.

[36] Zhiguo Zhao and Hua-Guang Gu. Transitions between classes of neuronal excitability and bifurcations induced by autapse. *Scientific Reports*, 7, 12 2017.